Glucocorticoid receptor over-expression promotes human small cell lung cancer apoptosis *in vivo* and thereby slows tumor growth

Paula Sommer, Rachel L Cowen[2], Andrew Berry[1], Ann Cookson[1], Brian A Telfer[2], Kaye J Williams[2], Ian J Stratford[2], Paul Kay[1], Anne White[1,3] and David W Ray[1,3]

School of Biological Sciences, University of KwaZulu-Natal, Westville Campus, Durban 4001, South Africa
[1]Endocrine Sciences Research Group, [2]School of Pharmacy and Pharmaceutical Sciences, Faculty of Medical and Human Sciences and [3]Faculty of Life Sciences, University of Manchester, AV Hill Building, Manchester, M13 9PT, UK

(Correspondence should be addressed to D W Ray; Email: david.w.ray@manchester.ac.uk;
A White; Email: anne.white@manchester.ac.uk)

Abstract

Small cell lung cancer (SCLC) is an aggressive tumor, associated with ectopic ACTH syndrome. We have shown that SCLC cells are glucocorticoid receptor (GR) deficient, and that restoration of GR expression confers glucocorticoid sensitivity and induces apoptosis *in vitro*. To determine the effects of GR expression *in vivo*, we characterized a mouse SCLC xenograft model that secretes ACTH precursor peptides, and so drives high circulating corticosterone concentrations (analogous to the ectopic ACTH syndrome). Infection of SCLC xenografts with GR-expressing adenovirus significantly slowed tumor growth compared with control virus infection. Time to fourfold initial tumor volume increased from a median of 9 days to 16 days ($P=0.05$; $n=7$ per group). Post-mortem analysis of GR-expressing tumors revealed a threefold increase in apoptotic (TUNEL positive) cells ($P<0.01$). Infection with the GR-expressing adenovirus caused a significant reduction in Bcl-2 and Bcl-xL transcripts. Furthermore, in both the GR-expressing adenovirus-infected cells and tumors, a significant number of uninfected cells underwent apoptosis, supporting a bystander cell killing effect. Therefore, GR expression is pro-apoptotic for human SCLCs *in vivo*, as well as *in vitro*, suggesting that loss of GR confers a survival advantage to SCLCs.

Endocrine-Related Cancer (2010) **17** 203–213

Introduction

Lung cancer is the most frequently diagnosed major cancer and the leading cause of cancer deaths worldwide. Small cell lung cancer (SCLC) comprises 20% of all lung cancers and is strongly associated with cigarette smoking. It is the most aggressive of the lung cancer subtypes and is generally disseminated at the time of diagnosis. While it is initially responsive to chemotherapy, the 5-year survival rate is $<5\%$ due to relapse with chemoresistant disease, resulting in a very poor prognosis (Jackman & Johnson 2005). Even though considerable advances have been made in the diagnosis and treatment of SCLCs over the past 10 years, long-term survival remains rare, and thus novel approaches to treatment are demanded. SCLCs are neuroendocrine carcinomas able to secrete a variety of ectopic neuropeptides including the ACTH precursor, proopiomelanocortin. The ectopic secretion of ACTH precursors by SCLCs has been shown to be resistant to normal negative feedback inhibition by circulating glucocorticoids (Gcs), which is evidence of Gc resistance (White *et al*. 1990, White & Clark 1993).

Gcs are vital steroid hormones with wide-ranging effects on cells and tissues, playing key roles in diverse

 DOI: 10.1677/ERC-09-0241
1351–0088/10/017–203

actions such as development and immunosuppression. Their action is mediated by the glucocorticoid receptor (GR) which belongs to the nuclear receptor superfamily. The inability of Gcs to inhibit ACTH precursor expression in SCLCs prompted investigation of GR expression in SCLCs. We (Ray *et al*. 1996, Sommer *et al*. 2007) and others (Hofmann *et al*. 1995) have shown that SCLC cells contain negligible amounts of functional GR, and hypothesized this to be the cause of Gc resistance. The human GR is a transcription factor that is expressed in virtually all cells and displays genome-wide action, influencing around 20% of the expressed genome (Donn *et al*. 2007). Activation by Gc ligand results in transcriptional induction or repression (Lu & Cidlowski 2006), and in addition, the GR is able to mediate less well-characterized non-genomic effects (Limbourg & Liao 2003, Matthews *et al*. 2008). Gcs, acting through the GR, have diverse effects on the survival of tissues and cell types, but transcriptional regulation by the GR is essential for life as $GR^{-/-}$ mice die shortly after birth (Reichardt *et al*. 1998).

Pertinent to this study, Gcs induce massive apoptosis in lymphoid cells, and thus are used as for the treatment of hematological malignancies. Despite being the subject of much study, a canonical pathway for GR-induced apoptosis has not been described and the mechanisms may vary between cell types (Herr *et al*. 2007). The requirement for sufficient levels of functional GR to induce apoptosis has been demonstrated in transgenic mice with increased or decreased GR expression in human acute lymphoblastic leukemia (T-ALL) cells expressing differing GR levels and in Gc-resistant and Gc-sensitive multiple myeloma cells (Schmidt *et al*. 2004). In $GR^{dim/dim}$ mice, in which the GR is unable to dimerize and therefore unable to bind to DNA, normal Gc-induced thymocyte apoptosis does not occur, suggesting that Gc-induced apoptosis involves *de novo* gene expression (Reichardt *et al*. 1998). However, gene expression analysis has revealed that some of the events leading to apoptosis may be activated by the non-genomic actions of the GR (Herr *et al*. 2007).

We have recently discovered that restoration of GR expression in human SCLC cells *in vitro* powerfully induces apoptosis (Sommer *et al*. 2007), suggesting that loss of GR expression in SCLC cells promotes their survival. Transgenic GR expression, which induced apoptotic cell death in SCLC cells, also upregulated pro-apoptotic genes of the Bcl-2 family (Sommer *et al*. 2007). The Bcl-2 family of proteins tightly regulates apoptosis, with damage signals being transduced by the BH3-only proteins (tBid, Bad, Bim, Noxa, and Puma) which interact with pro-survival family members (Bcl-2, Bcl-xL, Bcl-w, A1, and Mcl-1) to ablate their pro-survival function. This ablation allows activation of Bax and Bak which commit the cell to apoptosis (Adams & Cory 2007).

We have now extended our previous studies which showed that GR over-expression kills human SCLC cells *in vitro*, by assessing the impact of infecting tumors *in vivo* with GR-expressing adenoviral vectors. We now show that intratumoral injection of adenoviral GR powerfully induces SCLC apoptosis *in vivo*. Importantly, we found that GR over-expression caused a significant slowing in tumor growth, together with a possible bystander effect. In contrast to *in vitro* findings that GR over-expression upregulated the pro-apoptotic genes, *Bad* and *Bax* (Sommer *et al*. 2007), in the *in vivo* environment, GR over-expression downregulated the pro-survival genes, *Bcl-2* and *Bcl-xL*.

Materials and methods

Cell culture

DMS 79 cells (a gift from Prof. O Pettengill, Dartmouth Medical School, Hanover, NH, USA) were grown in RPMI-1640 medium containing glutamax (Gibco) supplemented with 10% (FBS) fetal bovine serum (Gibco) and 10 mM Hepes (Gibco). A549 and human embryonic kidney (HEK) 293 cells (ECACC, Porton Down, Wilts, UK) were cultured in DMEM (Gibco) containing glutamax supplemented with 10% FBS.

Viral vector construction and propagation

The AdEasy Adenoviral Vector System (Stratagene, La Jolla, CA, USA) was used to produce adenoviral vectors carrying GR-eYFP and eYFP. Briefly, GR-eYFP and eYFP were excised from pFUNC1 GR-eYFP and pFUNC1 eYFP (Sommer *et al*. 2007) using *Not1* and were subcloned into pShuttle-CMV. Successfully ligated pShuttle-CMV was linearized with *Pme1* and co-transformed with pAdEasy-1 supercoiled vector into BJ5183 competent cells. Recombination of pAdEasy-1 and ligated pShuttle-CMV was detected by *Pac1* digestion. Recombinant adenoviral plasmid was amplified by transformation into XL10-gold cells. Linearized recombinant adenoviral plasmids were transfected into permissive HEK 293 cells allowing homologous recombination and the generation of recombinant adenoviral vector particles. These were tested for efficacy by infecting A549 cells and determining the expression of GR and eYFP by real-time quantitative PCR. Large-scale preparations

of recombinant Ad-GR-eYFP and Ad-eYFP were prepared and purified using the Adeno-X virus purification kit (Clontech) and the viral titer was determined by plaque forming assays.

Adenoviral infection of A549 and DMS 79 cells

A549 and DMS 79 cells were infected at varying multiplicities of infection (MOIs: equivalent to plaque forming units/tumor cell). A549 cells grow as a monolayer and were infected by the addition of virus at MOIs of 10, 50, and 100 to the medium. DMS 79 cells grow as spheroids in suspension and so were transduced by spinning cells and virus at 2000 ***g*** for 2 h on two consecutive days in the presence of 8 μg/ml polybrene (Sigma).

Flow cytometry

DMS 79 cells at a density of $3–4\times10^6$ cells/ml were drawn up through a 0.4 mm×12 mm needle and expelled through a 40-μm cell strainer into PBS (BD Falcon, Le Pont declaix, France) to create a single cell suspension. Cells were analyzed for eYFP fluorescence (530/40 nm; infected cells) on a DakoCytomation Cyan flow cytometer using Summit software (DakoCytomation, Ely, UK). To determine viability, cells were stained with propidium iodide (PI) and gated to determine the percentage of eYFP- and PI-positive cells. For the apoptosis assays, the pelleted cells were resuspended in buffer (10 mM Hepes, 10 mM NaOH, 140 mM NaCl, and 25 mM $CaCl_2$), strained, incubated with 5-μl human recombinant APC-conjugated Annexin V (Bender MedSystems, Vienna, Austria) at room temperature for 15 min, and analyzed at 665/20 nm. To determine the percentage of eYFP-and Annexin V-positive cells, 10 000 cells were gated.

Xenograft studies

Low-passage number DMS 79 cells were grown to logarithmic phase. The cell concentration was adjusted to 1×10^8 cells/ml in serum-free RPMI-1640 medium and diluted to 5×10^7 cells/ml with the addition of matrigel (1:1; BD Biosciences, Cowley, UK). Xenografts were established by the s.c. injection of DMS 79 cells (0.1 ml, 5×10^7 DMS 79 cells in matrigel (1:1)) on the backs of female cba *nu/nu* mice. Once the tumors were established, measurements were made every 2–3 days using calipers. When the tumor size reached 180–200 mm^3, 5×10^8 pfu of control (Ad-eYFP) or Ad-GR-eYFP virus was delivered by intratumoral injection into the center of the tumor.

For the first experiment ($n=6$ per group), the tumors were excised 72 h after the initial injection and snap frozen. The spleen, kidneys, and adrenals were removed and placed into formalin fixative. The liver was snap frozen and the blood was collected.

For the growth delay experiment ($n=7$ per group), the virus was administered when the tumors reached 180–200 mm^3 in size, and twice thereafter at 4-day intervals. Tumor size was measured daily using calipers until their sizes reached four times the initial treatment size (RTV4), whereupon the tumors were harvested as described. Tumor growth delay was measured by plotting the average tumor size and S.E.M. per day. The time taken for each tumor to reach RTV4 was calculated, and the data were log transformed to overcome the non-parametric data and subjected to a two-tailed *t*-test.

All procedures were carried out using approved protocols (Home Office Project License 4002328) in accordance with the Scientific Procedures Act 1986 and in line with the United Kingdom Co-ordinating Committee on Cancer Research Guidelines on the welfare of animals in experimental neoplasia (Workman *et al*. 1988).

ACTH precursor and corticosterone assays

ACTH precursors were measured using a specific two-site ELISA based on an IRMA format described previously (Crosby *et al*. 1988). Corticosterone was measured using an ELISA with a sensitivity of 0.17 ng/ml (IDS Ltd).

Immunohistochemistry

Eight-micrometer tumor cryosections were fixed in 4% paraformaldehyde (PFA) for 15 min at room temperature. The sections were washed with PBS, permeabilized with 0.1% Triton X-100 in 0.1% sodium citrate in water for 2 min, washed with PBS, and blocked with 10% horse serum in PBS for 1.5 h at room temperature. To detect the presence of virus using eYFP, rabbit polyclonal green fluorescent protein (GFP) antibody (Invitrogen, 1:2000) was added to the sections at 4 °C overnight. The sections were then washed and incubated in FITC-labeled secondary anti-rabbit (Invitrogen, 1:500) for 1.5 h, following which, the sections were washed with PBS and mounted using hard set mounting medium containing 4',6-diamidino-2-phenylindole (DAPI) (Vector Labs). For co-localization with TUNEL staining, TUNEL reagent (TMR Red, Roche, Peterborough, UK) was added with the secondary antibody for 1.5 h in the dark at room temperature.

Positive and negative controls were set up as per the manufacturer's instructions. The images were captured on a Leica SP2 AOBS confocal microscope. The fluorescence intensity of TUNEL and GFP staining in ten sections was enumerated using Image J, and is presented as a ratio of TUNEL/GFP.

Quantitative PCR

Seventy-two hours post infection, RNA was extracted from DMS 79, A549, and HEK 293 cells spinfected or infected with GR-eYFP or eYFP viruses (RNeasy kit, Qiagen) as well as from tumors injected with Ad-eYFP or Ad-GR-eYFP (TriReagent, Sigma). After DNAse 1 treatment (Promega), cDNA was synthesized using Superscript 111 (Invitrogen) and Oligo-dT primers (Invitrogen). Quantitative PCR was performed using SYBR Green JumpStart Taq ready mix (Sigma) as per the manufacturer's instructions. Results were analyzed using the $2^{-\Delta\Delta C_t}$ method relative to GAPDH expression (Livak & Schmittgen 2001). Primer sequences are as follows: Bcl-2 (NM_000633.2) F 5′-CCCTCCAGATAGCTCATT-3′, R 5′-CTAGACAGACAAGGAAAG-3′; Bcl-xL (NM_001191.2) F 5′-ATCAATGGCAACCCATCCTG-3′, R 5′-TTGTCTACGCTTTCCACGCA-3′; Bin EL (NM_138621.3) F 5′-GCCACCTGCCAGC-3′, R 5′-ACAGCAGGGAGGATCTTCTCATAA-3′; GAPDH (NM_000012) F 5′-GAAGGTGAAGGTCGGAGT-3′, R 5′-GAAGATGGTGATGGGATTTC-3′; GRα (NM_000176) F 5′-CCATTGTCAAGAGGGAAGGA-3′, R 5′-CAGCTAACATCTCGGGGAGGAAT-3′; and eYFP F 5′-TGCTTCAGCCGCTACCCCGACC-3′, R 5′-CGCCGATGGGGGTGTTCTGCTG-3′.

To determine the number of successfully transfected cells per tumor, the number of eYFP transcripts in each tumor was calculated relative to eYFP expression in HEK where 100% of the cells were infected (as determined microscopically and by flow cytometry). Quantitative PCR was performed using primers for eYFP and GAPDH on tumor cDNA and HEK cDNA. The fold change in eYFP transcripts relative to GAPDH was calculated using the $2^{-\Delta\Delta C_t}$ method, and the data were changed to a percentage.

Statistical analysis

As the data on tumor growth were not normally distributed, they were log transformed and then comparisons were made using Student's *t*-test, two-tailed for independent samples. ACTH precursors and qRT-PCR were compared using an unpaired Student's *t*-test. Analyses were run using SPSS.

Results

SCLC xenografts

DMS 79 cells were used for xenograft generation because they secrete ACTH precursor peptides (a frequent clinical feature of human SCLCs), providing a potential biomarker for tumor presence or mass (White *et al*. 1990). DMS 79 cell xenografts exhibited typical SCLC pathology, and the mice had marked increases in circulating ACTH precursor concentrations (Fig. 1A and B). This was accompanied by adrenal cortical hyperplasia (data not shown). Engrafted mice also had raised corticosterone concentrations (180 ng/ml $\pm$ 64.5 for Ad-eYFP-injected tumors and 186 ng/ml $\pm$ 40 for Ad-GR-eYFP-injected tumors compared to 85.4 ng/ml $\pm$ 16.5 in non-engrafted animals), as predicted from the raised ACTH peptide concentrations, providing an accurate model of the ectopic ACTH syndrome.

Development of adenoviral vectors for GR-eYFP and eYFP

Previously, we had shown that retrovirally mediated over-expression of GR-eYFP in SCLC cell lines *in vitro* resulted in apoptotic cell death when compared with the effects of a control virus expressing eYFP alone (Sommer *et al*. 2007). However, effects on pure cell populations *in vitro* may not translate into the complex environment of a solid tumor, with vascular and cell matrix components influencing the tumor cells. Therefore, to determine what effect GR expression had on tumors, GR-eYFP and eYFP were cloned into adenoviral expression vectors to increase infection efficiency *in vivo*.

A549 and DMS 79 cells were infected with adenoviruses expressing eYFP alone or GR-eYFP at MOIs of 10, 50. and 100. Infection at all MOIs showed a significant upregulation of GR expression in all cells infected with Ad-GR-eYFP (Fig. 1C, MOI = 50). In the A549 cells, which are readily infected by adenovirus, a 1200-fold increase in GR expression was achieved. DMS 79 cells grow as spheroids in suspension and are notoriously difficult to transfect; however, infection with the GR-expressing adenovirus still resulted in a 400-fold increase in GR expression (Fig. 1C) and in an infection efficiency $>30\%$, as estimated using a simple eYFP-expressing adenovirus, a more reliable marker of infection as GR over-expression results in cell death (Fig. 1D).

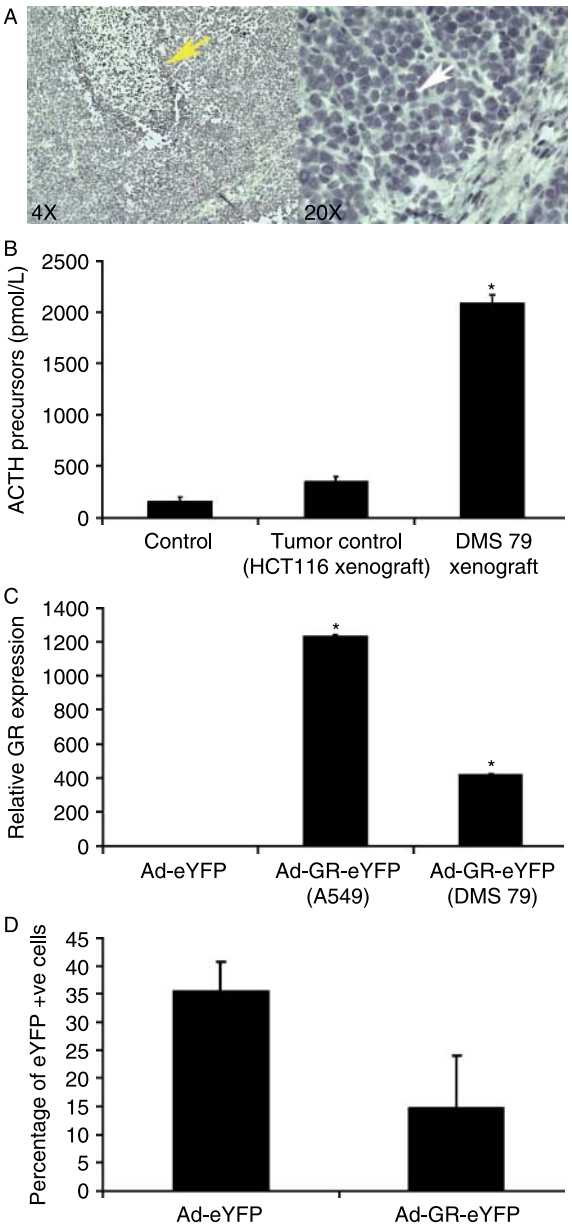

Figure 1 Development of SCLC xenografts in nude mice and functional testing of adenoviral vectors expressing *GR-eYFP* or *eYFP*. (A) SCLC xenografts were created by the s.c. injection of DMS 79 cells in matrigel. The SCLC xenografts displayed pathology that was similar to that of human SCLCs with large areas of necrosis (yellow arrow) and oval nuclei with scant cytoplasm (white arrow). (B) In addition, these tumors secreted ACTH precursors into the circulation at a higher level than non-SCLC human colon carcinoma xenografts (HCT116 cells; $n=3$, $^*P<0.05$). (C) Infection of A549 and DMS 79 cells with Ad-GR-eYFP resulted in a significant upregulation of GR expression when compared with GR expression in cells infected with the control virus, Ad-eYFP (MOI=50; $^*P<0.05$). (D) DMS 79 cells were spinfected with Ad-eYFP or Ad-GR-eYFP, and after 72 h, the percentage of infected (eYFP +ve) cells in each population was determined by FACS.

Ad-GR-eYFP infection of SCLC xenografts resulted in apoptotic death of infected cells *in vivo*

When SCLC xenografts reached 180–200 mm^3 in size, the tumors were injected with Ad-eYFP or Ad-GR-eYFP and were excised 72 h later ($n=6$ per group). As the eYFP fluorescence in the 8-μm sections was faint, the presence of eYFP was detected using an antibody. SCLC xenografts were successfully infected with the adenoviral vectors (Fig. 2A). There were more apoptotic cells, and a higher ratio of TUNEL-positive to eYFP-positive cells in tumors infected with the Ad-GR-eYFP adenovirus compared with tumors infected with the control virus, Ad-eYFP (Fig. 2A and B). PBS injection had no effect on apoptosis, and as expected, the resulting tumors were negative for eYFP expression (Fig. 2A).

As adenoviral delivery of transgenes is a relatively inefficient process (Krasnykh *et al*. 2000) which depends upon viral diffusion from the injection site, we estimated the number of successfully infected cells/tumor by enumerating the number of eYFP transcripts/tumor. RNA was extracted from tumors infected with control and Ad-GR-eYFP viruses. eYFP transcripts were amplified using real-time quantitative PCR and compared with eYFP expression in the HEK cell line (relative to GAPDH expression), where 100% of the cells were infected with the virus. There were consistently fewer eYFP-positive cells seen in tumors after GR-eYFP infection, probably due to death of infected cells (Fig. 2C).

Ad-GR-eYFP infection of SCLC xenografts in nude mice causes tumor growth delay

The *in vivo* effects of GR expression on the growth of the SCLC tumors were determined by injecting the GR-eYFP- and control eYFP-expressing adenoviral constructs when the established tumors had reached 180–200 mm^3 in size. Thereafter, the tumors were given two more injections at 4-day intervals and were harvested when the tumor volume had quadrupled (RTV4). Over-expression of the GR delayed tumor growth by 1 week (tumors infected with Ad-eYFP took 9 days to quadruple in size, whereas tumors infected with Ad-GR-eYFP took 16 days) ($t=2.131$, df=12, $P=0.05$) ($n=7$) (Fig. 3A and B). The wet weights of the adrenal glands, spleen, and kidneys were not changed (data not shown).

There was continuing expression of the viral transgenes at tumor harvest, but the proportion of eYFP-positive cells was lower after the injection of Ad-GR-eYFP than after the injection of Ad-eYFP alone, which was compatible with the loss of

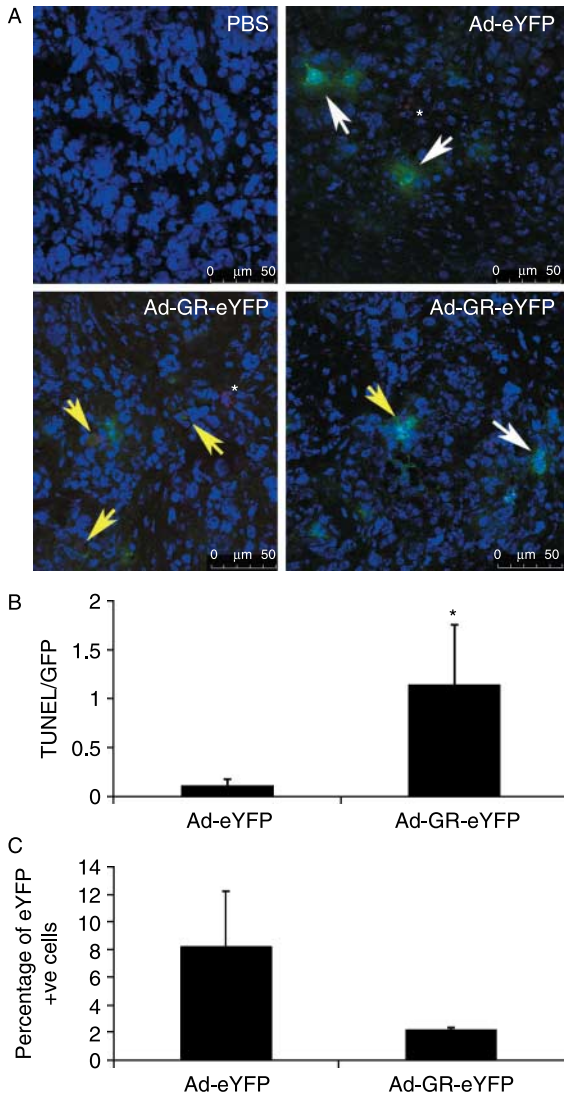

Figure 2 Ad-GR-eYFP infection of established SCLC xenografts resulted in apoptosis. (A) SCLC xenografts were injected with Ad-eYFP or Ad-GR-eYFP when the tumors reached 180–200 mm^3 in size ($n=6$ per group). After 72 h, the tumors were harvested. Cryosections were stained with anti-GFP (Invitrogen) to detect the presence of virus and with TUNEL-TMR (red; Roche) to detect apoptotic cells and were examined by confocal microscopy. No GFP or TUNEL staining was seen in tumors injected with PBS. GFP staining revealed cells infected with Ad-eYFP or Ad-GR-eYFP (white arrows), while apoptotic cells were revealed by TUNEL staining (*). Co-staining with GFP and TUNEL was clearly seen in Ad-GR-eYFP-infected cells only (yellow arrows). The two Ad-GR-eYFP panels represent two different fields for the same experimental conditions. (B) The total GFP and TUNEL fluorescence of ten different sections for each treatment was quantified using Image J software and is displayed as a ratio of TUNEL/GFP. Cells infected with Ad-GR-eYFP displayed significantly more TUNEL staining than cells infected with the control virus, Ad-eYFP (*$P<0.05$). (C) The percentage of eYFP-positive cells remaining in the tumors after 72 h was determined by real-time quantitative PCR and compared with eYFP expression in HEK cells, where 100% of the cells express eYFP.

GR-expressing cells (Fig. 3C). Importantly, even with relatively fewer GR-eYFP-positive cells being identified in tumor sections, over-expression of the GR caused a delay in tumor growth, suggesting a biologically important effect.

Ad-GR-eYFP infection of SCLC xenografts in nude mice induces tumor cell apoptosis

To investigate the effect of GR expression on growth rate, tumor sections were analyzed by TUNEL staining. There was evidence of a greatly increased rate of apoptosis in tumors infected with Ad-GR-eYFP compared with the Ad-eYFP control (Fig. 3D and E). A clear increase in the amount of TUNEL staining is seen in tumors injected with Ad-GR-eYFP (Fig. 3E) when compared with Ad-eYFP-injected xenografts (Fig. 3D) quantified in Fig. 3F.

Ad-GR-eYFP infection of SCLC xenografts also results in apoptosis of uninfected tumor cells: a bystander effect?

The increased TUNEL staining in both infected and uninfected cells in tumors injected with Ad-GR-eYFP coupled with the significant growth delay despite relatively low infection rates prompted us to investigate apoptosis *in vitro* in uninfected SCLC cells in mixed populations with infected Ad-GR-eYFP-expressing cells. Over-expression of GR by adenoviral infection caused the death of infected SCLC cells (yellow arrow) when compared with cells infected with control virus (Fig. 4A and B), which is an effect similar to that seen with retroviral gene delivery (Sommer *et al*. 2007). Interestingly, there is also a clear shift in the population of non-GR-eYFP-positive SCLC cells toward cell death (black arrow; Fig. 4B). We showed that there was a significant increase in cell death (Fig. 4C) and apoptosis (Fig. 4D) in non-GR-expressing cells derived from infected populations when quantified.

The same effect is seen *in vivo* where there was clearly more apoptosis in uninfected cells in xenografts exposed to Ad-GR-eYFP than in those exposed to the control, Ad-eYFP (Fig. 4E–G). The evidence suggests a bystander effect, whereby GR-induced cell death transmits a pro-apoptotic signal to non-expressing SCLC cells.

Ad-GR-eYFP infection of SCLC xenografts affects expression of pro-survival and pro-apoptotic genes

Previously, we had shown that, *in vitro*, over-expression of the GR caused a significant upregulation

of the pro-apoptotic genes, *Bad* and *Bax*, which resulted in apoptosis of the SCLC cell lines. Here, we show that the tumor microenvironment has a significant effect on gene expression. Bad (Fig. 5A) and Bim (Fig. 5B) are over-expressed in DMS 79 xenografts when compared with expression profiles *in vitro*. However, the expression of Bad *in vivo* is unaffected by GR over-expression. Bax levels are similar *in vivo* and *in vitro* and are unaffected by GR over-expression *in vivo* (Fig. 5C). Most notably, we showed that while DMS 79 cells express low levels of the pro-survival genes, *Bcl-2* and *Bcl-xL in vitro* (Fig. 5D and E), in the tumor microenvironment, the expression of Bcl-2 and Bcl-xL is dramatically upregulated and significantly repressed by over-expression of the GR.

Discussion

We have used a human SCLC xenograft model of lung cancer to analyze the effect of GR expression on tumor behavior. We have shown that over-expression of GR in these SCLC xenografts leads to apoptotic cell death associated with downregulation of the pro-survival genes, *Bcl-2* and *Bcl-xL*, and results in delayed tumor growth *in vivo*.

A

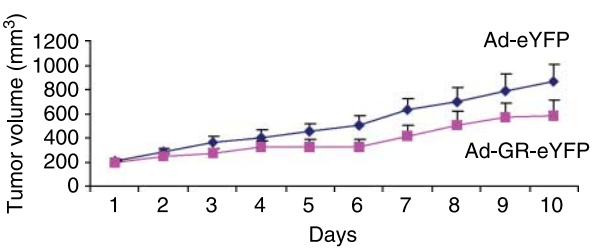

B

	Days taken for tumor to reach RTV4 Median (mean)
Ad-eYFP	9 (11)
Ad-GR-eYFP	16 (14.75)

$P < 0.05$, $n = 7$ per group

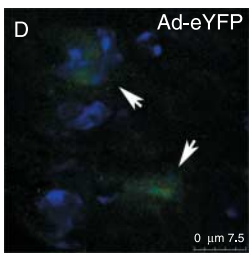

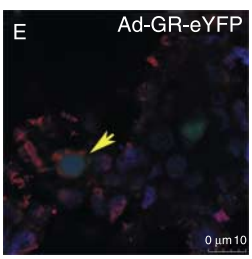

C

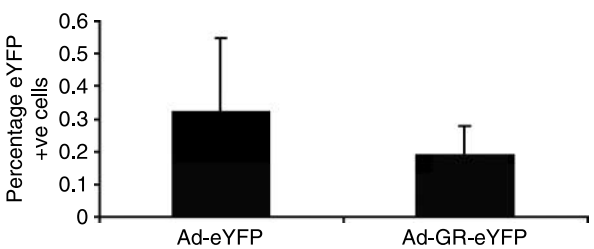

F

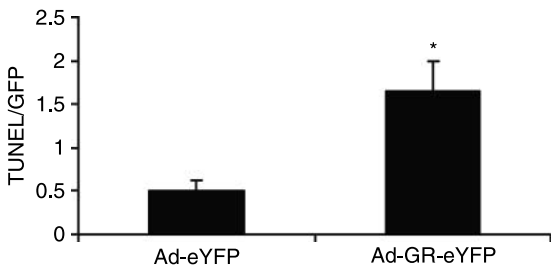

Figure 3 Infection of tumor cells with Ad-GR-eYFP caused growth delay. (A) When SCLC xenografts reached 180–200 mm^3 in size, the tumors were injected with either Ad-eYFP or Ad-GR-eYFP, three times at 4-day intervals ($n=7$ per treatment). Tumor growth was measured daily using calipers and the tumors were excised when the relative tumor volume reached four times the initial injection size. (B) Restored GR expression significantly ($P=0.05$) slowed tumor growth to four times the initial treatment size by 1 week. (C) To determine the number of infected cells per tumor, qPCR was used to determine the number of eYFP transcripts from three tumors. The percentage of eYFP-positive cells in the tumors at harvest was compared with eYFP expression in HEK cells, where 100% of the cells express eYFP relative to GAPDH expression. Growth delay caused by Ad-GR-eYFP is mediated by increased apoptosis. (D–F) Cryosections were stained with anti-GFP (Invitrogen) to detect the presence of virus and with TUNEL-TMR (red; Roche) to detect apoptotic cells and were examined by confocal microscopy. Although Ad-eYFP was effective in infecting tumor cells (white arrows) (D), few TUNEL-positive tumor cells were seen in the representative sections shown. However, tumor cells infected with Ad-GR-eYFP also stained positive with TUNEL (E) (yellow arrows). (F) The total GFP and TUNEL fluorescence of ten different sections for each treatment was quantified using Image J software and is displayed as a ratio of TUNEL/GFP. Cells infected with Ad-GR-eYFP displayed significantly more TUNEL staining than cells infected with the control virus, Ad-eYFP (*$P<0.05$).

Previously, we had shown that the SCLC cell line (DMS 79) used to create the xenograft model expressed very low levels of the GR, and that restoration of GR expression in the cells by transfection inhibited the secretion of ACTH precursors from the cells in culture (Sommer *et al*. 2007). In this study, we found that tumors formed from DMS 79 cells also secreted ACTH precursor peptides. The excess ACTH precursor peptides in the circulation mimicked the ectopic ACTH syndrome and resulted in hyperplasia of the corticosterone-producing cells in the zona fasciculata of the adrenal cortex, as expected, but there was no significant change in adrenal wet weight, possibly reflecting the relatively short exposure of the adrenal glands to ACTH drive. Restoration of GR expression by infection of Ad-GR-eYFP in the xenografts did not inhibit plasma ACTH precursor peptides or circulating corticosterone. This may reflect the protocol design, given that samples were not collected until the tumor was removed, which was done at a time when tumor burden ($\sim$800 mm^3) was similar in the eYFP and GR-eYFP groups.

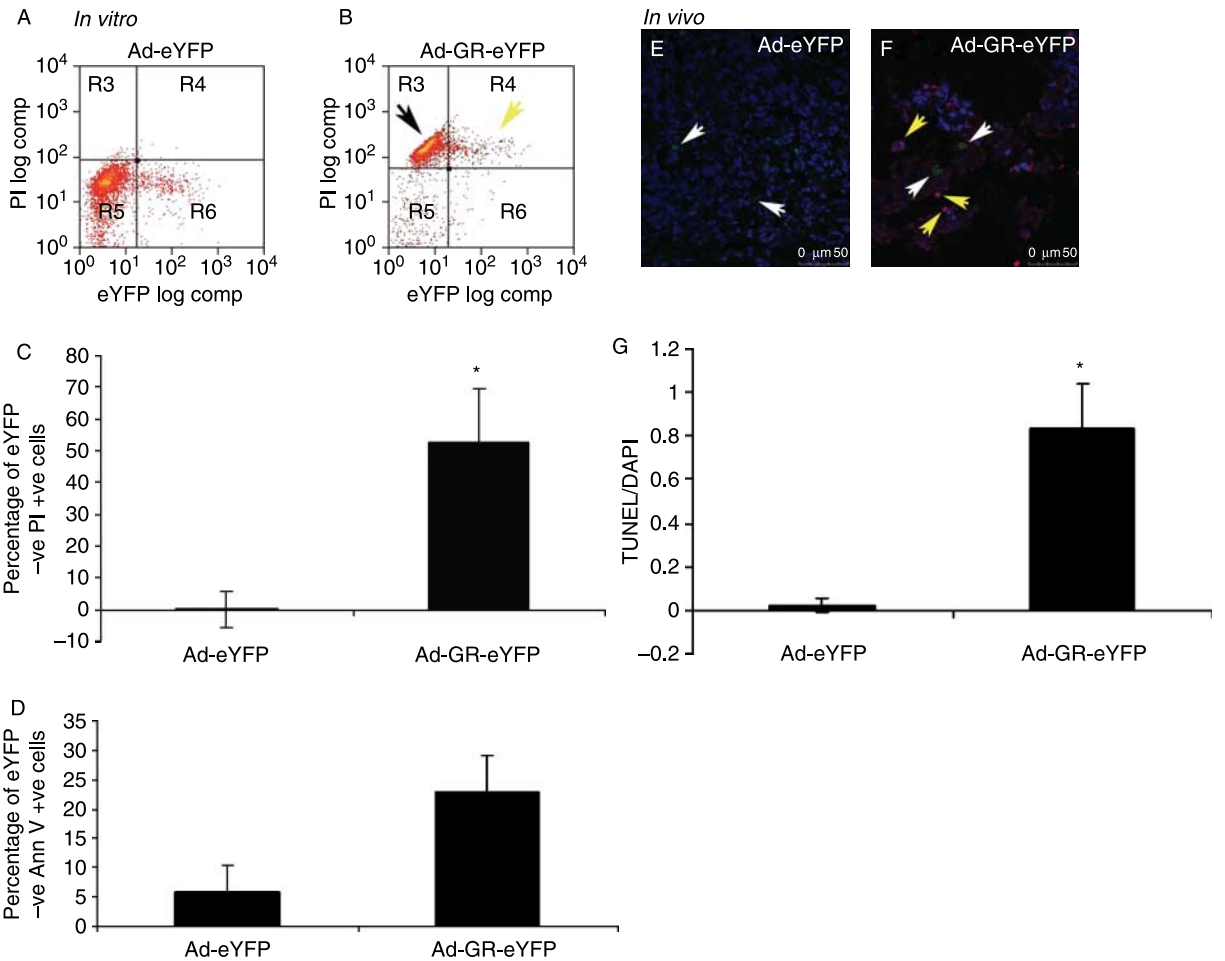

Figure 4 Apoptosis in DMS 79 cells and xenografts infected with Ad-GR-eYFP. *In vitro*: DMS 79 cells were infected with adenovirus. After 72 h, the cells were stained with PI and Annexin V and analyzed by flow cytometry. There is a clear shift in the Ad-GR-eYFP-infected population toward a dead or dying state (yellow arrow) (B) compared with the control virus-infected cells (A). There is also a similar shift in non-GR-eYFP-expressing cells (black arrow) (B). Ad-eYFP serves as a control where no such shift is seen (A). The proportion of uninfected (eYFP −ve) cells, drawn from the same populations described above, which are PI +ve (C) and AnnV +ve is shown (D). In C and D, a mean ($\pm$S.D.) of three separate experiments is shown (*$P<0.05$, compared with eYFP control). *In vivo*: tumor cryosections were stained with anti-GFP (Invitrogen) to detect the presence of virus and with TUNEL-TMR (red; Roche) to detect apoptotic cells and were examined by confocal microscopy. Ad-eYFP- and Ad-GR-eYFP-infected cells can be seen clearly (white arrows, E and F respectively). Little or no TUNEL staining is seen in the Ad-eYFP-injected xenograft. However, TUNEL staining is clearly visible in non-GR-eYFP-expressing cells in the Ad-GR-eYFP-infected tumor (yellow arrows, F). (G) The amount of TUNEL fluorescence in ten different sections from three different Ad-eYFP and Ad-GR-eYFP was quantified using Image J software (*$P<0.05$).

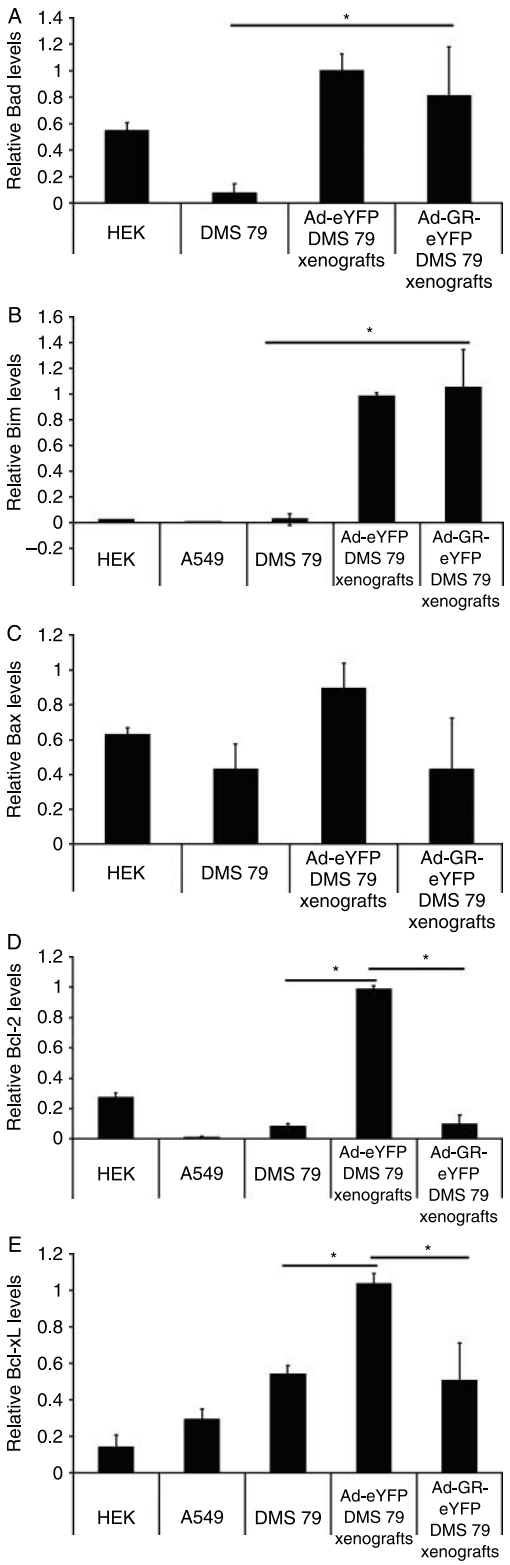

It is important to note that there was high circulating corticosterone in all SCLC xenograft-bearing animals capable of activating the transgenic GR.

Ad-eYFP and Ad-GR-eYFP were shown to infect tumor cells by immunostaining for the presence of eYFP. Infection with Ad-GR-eYFP resulted in apoptotic death of the SCLC tumor cells as evidenced by TUNEL assay. Mitochondrial apoptosis is regulated via a balance between the BH3-only pro-apoptotic proteins (such as Bad, Bim, Bid, Noxa, and Puma) and the pro-survival proteins (such as Bcl-2 and Bcl-xL). Cell survival is promoted by elevated levels of pro-survival proteins such as Bcl-2 and Bcl-xL, which prevent Bax-mediated perturbation of the mitochondrial membrane (Adams & Cory 2007) and thus inhibit apoptosis. Resistance to therapy in multiple cancers is associated with over-expression of Bcl-2 and Bcl-xL (Olejniczak *et al*. 2007, Schwartz *et al*. 2007). Bcl-2 is over-expressed in 75% of the SCLCs (Pisick *et al*. 2003), and its locus is amplified in 48% of the patients (Olejniczak *et al*. 2007). While the Bcl-2 locus in the DMS 79 cells used to create the xenografts is not amplified (Olejniczak *et al*. 2007), we found that the tumors over-expressed Bcl-2 as well as Bcl-xL, Bad, and Bim in comparison to transcript levels *in vitro*, while Bax levels remained unchanged. Most notably, over-expression of GR by adenoviral infection in these tumors significantly inhibited Bcl-2 and Bcl-xL transcript abundance. These results are similar to those in the juvenile rat hippocampus, where dexamethasone has been shown to downregulate Bcl-2 and Bcl-xL and upregulate Bax (Sandau & Handa 2007), while downregulation of Bcl-2 expression is thought to contribute to Gc-induced apoptosis in U2-OS cells (Rogatsky *et al*. 1999, Lu *et al*. 2007). The mechanism whereby the GR regulates these genes remains unclear. Analysis of the promoter region and 5 kb upstream revealed potential GR binding sites in Bcl-xL but not in Bcl-2 (MatInspector, Genomatix, www.genomatix.de).

These results differ from our *in vitro* findings where over-expression of the GR increased Bad and Bax transcript abundance, suggesting that over-expression

Figure 5 Expression levels of pro-survival and pro-apoptotic genes in tumors injected with Ad-eYFP and Ad-GR-eYFP. Seventy-two hours post infection, RNA was extracted from DMS 79, A549, and HEK 293 cells spinfected or infected with Ad-GR-eYFP or Ad-eYFP viruses as well as from tumors injected with Ad-eYFP or Ad-GR-eYFP. cDNA was synthesized and subjected to real-time quantitative PCR. The relative expression levels of Bad (A), Bim (B), Bax (C), Bcl-2 (D), and Bcl-xL (E) are shown. Data were analyzed using the $2^{-\Delta\Delta C_t}$ method relative to GAPDH expression (*$P<0.05$; comparisons are shown with horizontal bars; $n=3$).

of the GR in SCLC cells results in apoptosis both *in vitro* and *in vivo*; however, the pro-apoptotic rheostat is activated *in vitro*, while the pro-survival rheostat is suppressed *in vivo*, illustrating the effect of the tumor microenvironment on gene expression. Here, we suggest that GR-mediated inhibition of Bcl-2 and Bcl-xL would relieve repression of Bax activity and thus trigger the apoptotic cascade, thereby slowing tumor growth. This effect has been shown previously where small molecule inhibitors of pro-survival proteins such as ABT-737 improved survival and caused tumor regression in mice (Oltersdorf *et al.* 2005, Tahir *et al.* 2007).

A major limitation of gene delivery using adenoviral vectors is the inability to transduce all the tumor cells *in vivo*. In this study, we have shown that only 8% of the tumor cells express the *eYFP* transgene, yet significant growth delay and changes in gene expression occur. Examination of sections of infected tumors revealed TUNEL staining in uninfected cells. These cells may have had low level expression of the transgene, or may have lost transgene expression after committing to the apoptotic program. However, the frequency of apoptotic cells in Ad-GR-eYFP-injected tumors is greater than the predicted frequency of transgene-expressing cells, based on the experiments with the Ad-eYFP-injected tumors. Indeed, both retroviral delivery of GR (Sommer *et al.* 2007) and adenoviral delivery to SCLC cells *in vitro* resulted in a striking excess of apoptotic cells compared with the number found to be expressing the transgene. As the number of dying cells seen in GR-eYFP-infected cell cultures is greater than the number of cells estimated to be infected (eYFP positive after eYFP adenoviral infection), this supports a bystander cell kill effect.

Bystander killing plays a crucial role in cancer therapy as it significantly amplifies the anti-tumor effect of cytotoxic therapy (Hyer *et al.* 2003). This has been observed in response to u.v. radiation, photodynamic therapy, and chemotherapeutic agents in diverse cell types such as lymphocytes, fibroblasts, endothelial cells, and tumor cells. Despite the importance of this phenomenon, the mechanisms that are responsible are poorly defined (Prise & O'Sullivan 2009). *In vitro* analysis suggests two mechanisms. For cells in direct contact, small molecules, including secondary messengers, can transmit apoptotic signals through gap junctions. Alternatively, the release of 'death' signals into the extracellular fluid may stimulate cells not in direct contact to undergo apoptosis. The latter mechanism is well documented in response to radiation, but the nature of the signal(s) remains unknown (Prise & O'Sullivan 2009). Recently, mitochondria-mediated apoptosis has been shown to be able to induce a bystander effect *in vitro* whereby signals are transduced to neighboring cells via gap junctions, although again the nature of the signal has not been elucidated (Peixoto *et al.* 2009). Thus, it is possible that the bystander apoptosis seen in this study is mediated by transmission of apoptotic signals through gap junctions. However, it is clear that bystander responses are more complex, and harder to define in tumors grown *in vivo* (Prise & O'Sullivan 2009). Therefore, in our current study, which relies on solid tumor growth, both diffusion and gap junction mechanisms may play a role.

In conclusion, we report that over-expression of the GR in SCLC xenografts causes apoptotic death of the SCLC cells in tumor grafts by downregulation of pro-survival genes and thus significantly delays tumor growth. The pro-apoptotic effect of restored GR expression in SCLC cells *in vitro* and now *in vivo* is a novel and exciting finding, and a deeper understanding of the mechanism whereby GR causes apoptosis in these cells offers a great promise for developing more selective and efficacious therapeutic agents.

Declaration of interest

The authors declare that there is no conflict of interest that could be perceived as prejudicing the impartiality of the research reported.

Funding

P Sommer, A Berry, A Cookson, P Kay, A White, and D W Ray were funded by the Wellcome Trust. R L Cowen, B A Telfer, K J Williams, and I J Stratford were funded by the MRC. D W Ray was funded by the NIHR Manchester Biomedical Research Centre.

Acknowledgements

We are grateful to the Wellcome Trust for funding.

References

Adams JM & Cory S 2007 The Bcl-2 apoptotic switch in cancer development and therapy. *Oncogene* **26** 1324–1337.

Crosby SR, Stewart MF, Ratcliffe JG & White A 1988 Direct measurement of the precursors of adrenocorticotropin in human plasma by two-site immunoradiometric assay. *Journal of Clinical Endocrinology and Metabolism* **67** 1272–1277.

Donn R, Berry A, Stevens A, Farrow S, Betts J, Stevens R, Clayton C, Wang J, Warnock L, Worthington J *et al.* 2007 Use of gene expression profiling to identify a novel glucocorticoid sensitivity determining gene, BMPRII. *FASEB Journal* **21** 402–414.

Herr I, Gassler N, Friess H & Buchler MW 2007 Regulation of differential pro- and anti-apoptotic signaling by glucocorticoids. *Apoptosis* **12** 271–291.

Hofmann J, Kaiser U, Maasberg M & Havemann K 1995 Glucocorticoid receptors and growth inhibitory effects of dexamethasone in human lung cancer cell lines. *European Journal of Cancer* **31A** 2053–2058.

Hyer ML, Sudarshan S, Schwartz DA, Hannun Y, Dong JY & Norris JS 2003 Quantification and characterization of the bystander effect in prostate cancer cells following adenovirus-mediated FasL expression. *Cancer Gene Therapy* **10** 330–339.

Jackman DM & Johnson BE 2005 Small-cell lung cancer. *Lancet* **366** 1385–1396.

Krasnykh V, Dmitriev I, Navarro JG, Belousova N, Kashentseva E, Xiang J, Douglas JT & Curiel DT 2000 Advanced generation adenoviral vectors possess augmented gene transfer efficiency based upon coxsackie adenovirus receptor-independent cellular entry capacity. *Cancer Research* **60** 6784–6787.

Limbourg FP & Liao JK 2003 Nontranscriptional actions of the glucocorticoid receptor. *Journal of Molecular Medicine* **81** 168–174.

Livak KJ & Schmittgen TD 2001 Analysis of relative gene expression data using real-time quantitative PCR and the 2(−Delta Delta *C*(T)) method. *Methods* **25** 402–408.

Lu NZ & Cidlowski JA 2006 Glucocorticoid receptor isoforms generate transcription specificity. *Trends in Cell Biology* **16** 301–307.

Lu NZ, Collins JB, Grissom SF & Cidlowski JA 2007 Selective regulation of bone cell apoptosis by translational isoforms of the glucocorticoid receptor. *Molecular and Cellular Biology* **27** 7143–7160.

Matthews L, Berry A, Ohanian V, Ohanian J, Garside H & Ray D 2008 Caveolin mediates rapid glucocorticoid effects and couples glucocorticoid action to the antiproliferative program. *Molecular Endocrinology* **22** 1320–1330.

Olejniczak ET, Van Sant C, Anderson MG, Wang G, Tahir SK, Sauter G, Lesniewski R & Semizarov D 2007 Integrative genomic analysis of small-cell lung carcinoma reveals correlates of sensitivity to bcl-2 antagonists and uncovers novel chromosomal gains. *Molecular Cancer Research* **5** 331–339.

Oltersdorf T, Elmore SW, Shoemaker AR, Armstrong RC, Augeri DJ, Belli BA, Bruncko M, Deckwerth TL, Dinges J, Hajduk PJ *et al.* 2005 An inhibitor of Bcl-2 family proteins induces regression of solid tumours. *Nature* **435** 677–681.

Peixoto PM, Ryu SY, Pruzansky DP, Kuriakose M, Gilmore A & Kinnally KW 2009 Mitochondrial apoptosis is amplified through gap junctions. *Biochemical and Biophysical Research Communications* **390** 38–43.

Pisick E, Jagadeesh S & Salgia R 2003 Small cell lung cancer: from molecular biology to novel therapeutics. *Journal of Experimental Therapeutics and Oncology* **3** 305–318.

Prise KM & O'Sullivan JM 2009 Radiation-induced bystander signalling in cancer therapy. *Nature Reviews. Cancer* **9** 351–360.

Ray DW, Davis JR, White A & Clark AJ 1996 Glucocorticoid receptor structure and function in glucocorticoid-resistant small cell lung carcinoma cells. *Cancer Research* **56** 3276–3280.

Reichardt HM, Kaestner KH, Tuckermann J, Kretz O, Wessely O, Bock R, Gass P, Schmid W, Herrlich P, Angel P *et al.* 1998 DNA binding of the glucocorticoid receptor is not essential for survival. *Cell* **93** 531–541.

Rogatsky I, Hittelman AB, Pearce D & Garabedian MJ 1999 Distinct glucocorticoid receptor transcriptional regulatory surfaces mediate the cytotoxic and cytostatic effects of glucocorticoids. *Molecular and Cellular Biology* **19** 5036–5049.

Sandau US & Handa RJ 2007 Glucocorticoids exacerbate hypoxia-induced expression of the pro-apoptotic gene Bnip3 in the developing cortex. *Neuroscience* **144** 482–494.

Schmidt S, Rainer J, Ploner C, Presul E, Riml S & Kofler R 2004 Glucocorticoid-induced apoptosis and glucocorticoid resistance: molecular mechanisms and clinical relevance. *Cell Death and Differentiation* **11** (Suppl 1) S45–S55.

Schwartz PS, Manion MK, Emerson CB, Fry JS, Schulz CM, Sweet IR & Hockenbery DM 2007 2-Methoxy antimycin reveals a unique mechanism for Bcl-x(L) inhibition. *Molecular Cancer Therapeutics* **6** 2073–2080.

Sommer P, Le Rouzic P, Gillingham H, Berry A, Kayahara M, Huynh T, White A & Ray DW 2007 Glucocorticoid receptor overexpression exerts an antisurvival effect on human small cell lung cancer cells. *Oncogene* **26** 7111–7121.

Tahir SK, Yang X, Anderson MG, Morgan-Lappe SE, Sarthy AV, Chen J, Warner RB, Ng SC, Fesik SW, Elmore SW *et al.* 2007 Influence of Bcl-2 family members on the cellular response of small-cell lung cancer cell lines to ABT-737. *Cancer Research* **67** 1176–1183.

White A & Clark AJ 1993 The cellular and molecular basis of the ectopic ACTH syndrome. *Clinical Endocrinology* **39** 131–141.

White A, Clark AJ & Stewart MF 1990 The synthesis of ACTH and related peptides by tumours. *Bailliere's Clinical Endocrinology and Metabolism* **4** 1–27.

Workman P, Balmain A, Hickman JA, McNally NJ, Rohas AM, Mitchison NA, Pierrepoint CG, Raymond R, Rowlatt C, Stephens TC *et al.* 1988 UKCCCR guidelines for the welfare of animals in experimental neoplasia. *Laboratory Animals* **22** 195–201.